Scaling behavior and complexity of plastic deformation for a bulk metallic glass at cryogenic temperatures

Cun Chen,[1] Jingli Ren,[1,*] Gang Wang,[2] Karin A. Dahmen,[3] and Peter K. Liaw[4]

[1]*School of Mathematics and Statistics, Zhengzhou University, 100 Science Road, Zhengzhou 450001, China*

[2]*Laboratory for Microstructures, Shanghai University, Shanghai 200444, China*

[3]*Department of Physics and Institute of Condensed Matter Theory, University of Illinois at Urbana-Champaign, 1110 West Green Street, Urbana, Illinois 61801, USA*

[4]*Department of Materials Science and Engineering, University of Tennessee, Knoxville, Tennessee 37996, USA*

(Received 15 April 2015; published 8 July 2015)

We explore the scaling behavior and complexity in the shear-branching process during the compressive deformation of a bulk metallic glass $Zr_{64.13}Cu_{15.75}Al_{10}Ni_{10.12}$ (at. %) at cryogenic temperatures. The fractal dimension of the stress rate signal ranges from 1.22 to 1.72 with decreasing temperature and a larger shear-branching rate occurs at lower temperature. A stochastic model is introduced for the shear-branching process. In particular, at a temperature of 213 K, the shear-branching process evolves as a self-similar random process. In addition, the complexity of the stress rate signal conforms to the larger activation energy of the shear transformation zone at lower temperatures.

DOI: 10.1103/PhysRevE.92.012113 PACS number(s): 02.50.Fz, 05.45.Df, 81.05.Kf, 62.20.fk

To explore the plastic deformation mechanism during compressive deformation for bulk metallic glasses (BMGs), the serrated flow signal is usually discussed in terms of various methods, such as the chaotic time series analysis [1], the statistical analysis [1–4], and the spatiotemporal dynamic model [5–8]. The shear-band-slip avalanche is the dominant mechanism of plastic deformation in BMGs, which demonstrates the agreement between high-temporal-resolution measurements of the slip statistics and the dynamics of the predictions of a simple mean-field theory [9,10]. The multiple shear-band patterns show fractal characteristics in the severely deformed BMGs under specific loading conditions [11]. For the BMGs with good ductility, the dynamics of the serrated plastic flow manifests a self-organized criticality (SOC) state, which has a power-law scaling behavior [1].

Recently, a few of studies have focused on the deformation behavior of BMGs under extreme conditions, such as at cryogenic temperatures or high strain rates [12–16]. The shear-banding behavior and the plastic flow for the inhomogeneous deformation of BMGs are considered to be affected by deformation units [14]. The activation energy increment of the deformation units at lower temperatures is the main factor influencing the fracture strength of BMGs [17]. In fact, the plasticity of BMGs is unexpectedly improved with decreasing temperature [4,12]. However, the exact elucidation of how the temperature influences the plastic deformation of BMGs is still unclear. In the current work, the scale-free fractal behavior and the complexity information in the shear-branching process of a BMG are investigated to provide valuable information to further characterize the evolution of the shear bands and plastic deformation mechanism of BMGs at cryogenic temperatures since the intermittent serrated flow is not appropriate for the continuous system and the stress-time signal of metallic glasses appears quite complicated and irregular.

A $Zr_{64.13}Cu_{15.75}Al_{10}Ni_{10.12}$ (at. %) BMG is compressed in a temperature range from 133 to 305 K with a strain rate of $2.5 \times 10^{-4}\,s^{-1}$. The stress-time curves are established in Fig. 1, which shows that as the temperature decreases from 305 to 133 K, the amplitude of serrations reduces gradually and disappears at a temperature of 193 K. Clearly, there is a transition from the serrated to nonserrated plastic flow with decreasing temperature. Hence, it is required to investigate the plastic deformation mechanism based not only on the serrated flow but also on the nonserrated flow.

It was shown in previous works [18–21] that several degrees of short- and medium-range order did exist in BMGs, which means that there are self-similar characteristics hidden in BMGs. Xi *et al.* found a fractal-like dimpled structure on the fracture surface of a Ti-based BMG [22]. Sun and Wang further quantitatively analyzed the fractal characteristic of the two-dimensional fracture surface of Zr-based BMG [11]. The analysis based on the two-dimensional fracture surface reflects the local feature of the shear-branching process, for which the actual spread is in a three-dimensional space. Considering that it is difficult to measure shear bands distributed spatially, we focus our research on the temporal stress rate signal of $Zr_{64.13}Cu_{15.75}Al_{10}Ni_{10.12}$ BMG $\{d\sigma(i)/dt,\ i = 1,2,\ldots,N\}$ (see Fig. 2) because it reflects the global feature of the shear-branching process.

The calculation of the fractal dimension is, according to the box-counting method [23], based on the stress rate signal $\{x(i) = d\sigma(i)/dt,\ i = 1,2,\ldots,N\}$. Square boxes with a length of l can cover the total data set, which needs at least $N(l)$ boxes. Changing the box size l, we can obtain a series of $N(l)$. Fitting $[l, N(l)]$ in a double logarithmic plot, the slope of this fitting curve is expressed as

$$D = -\lim_{l\to 0} \frac{\ln N(l)}{\ln l}, \tag{1}$$

where D is the fractal dimension of the stress rate signal.

The fractal dimension D as a function of the temperature is plotted in Fig. 3. It can be seen that the D value increases

*Corresponding author: renjl@zzu.edu.cn

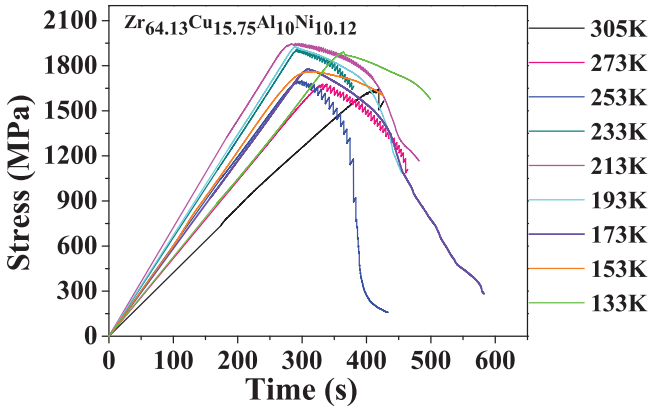

FIG. 1. (Color) Comparative stress-time curves for $Zr_{64.13}Cu_{15.75}Al_{10}Ni_{10.12}$ glassy metal deformed at different temperatures, 133, 153, 173, 193, 213, 233, 253, 273, and 305 K, with a strain rate of $2.5 \times 10^{-4}\ s^{-1}$.

with temperature decreasing from 305 to 133 K, suggesting an enhanced fractal behavior at low temperature. The largest D value appears at the temperature of 133 K, indicating the largest shear-branching rate. In this case, numerous shear bands with hierarchical structure can propagate in a scale-free manner. The fractal dimension of the shear-branching structure actually reflects the branching rates of a primary shear band evolving to the secondary shear band. The formation of the fractal structure results from the interactions among shear-band hierarchies located at different places and in different directions. For BMGs at lower temperatures with a larger fractal dimension, the plasticity is also improved, which is attributed to the concurrent nucleation of a large number of shear bands throughout the sample. The higher density of shear bands in turn can induce a hierarchical structure in the length scales of shear banding. Thus, a large number of shear bands usually are accompanied by the spread of the hierarchical structure. The shear-branching process includes short-range interactions from the intersection of the shear bands, the consequent arrest, and the long-range interaction of the strain fields initiated from different shear bands. Along with the shear-branching process, the serrated flow behavior is manifested in the plastic regime in the Zr-based BMG. Each stress drop in the serration event corresponds to the system surmounting the barrier and then jumping to a neighboring metastable state, which is believed to show SOC-type dynamics, especially at lower temperatures (the cryogenic level) [4].

Based on the stress rate signal $\{x(i) = d\sigma(i)/dt,\ i = 1,2,\ldots,N\}$, the detrended fluctuation analysis is used to quantify the evolution of the shear-branching structure. The process of the detrended fluctuation analysis is described as follows [24–27]. The signal $\{x(i),\ i = 1,2,\ldots,N\}$ is divided into N_q (where $N_q = N/q$) zones with each zone containing q elements. In the kth zone, the local trend is defined as a linear function of $\hat{x}_k(j)$, $j = 1,2,\ldots,q$, which is linearly fitted by the original series $x_k(j)$, $j = 1,2,\ldots,q$. The detrended time series is $x_k(j) - \hat{x}_k(j)$, $j = 1,2,\ldots,q$, with a mean-square error $F^2(k) = \frac{1}{q}\sum_{j=1}^{q}[x_k(j) - \hat{x}_k(j)]^2$. The root mean square is expressed as $F_q = [\frac{1}{N_q}\sum_{k=1}^{N_q} F^2(k)]^{1/2}$ in the total N_q zones,

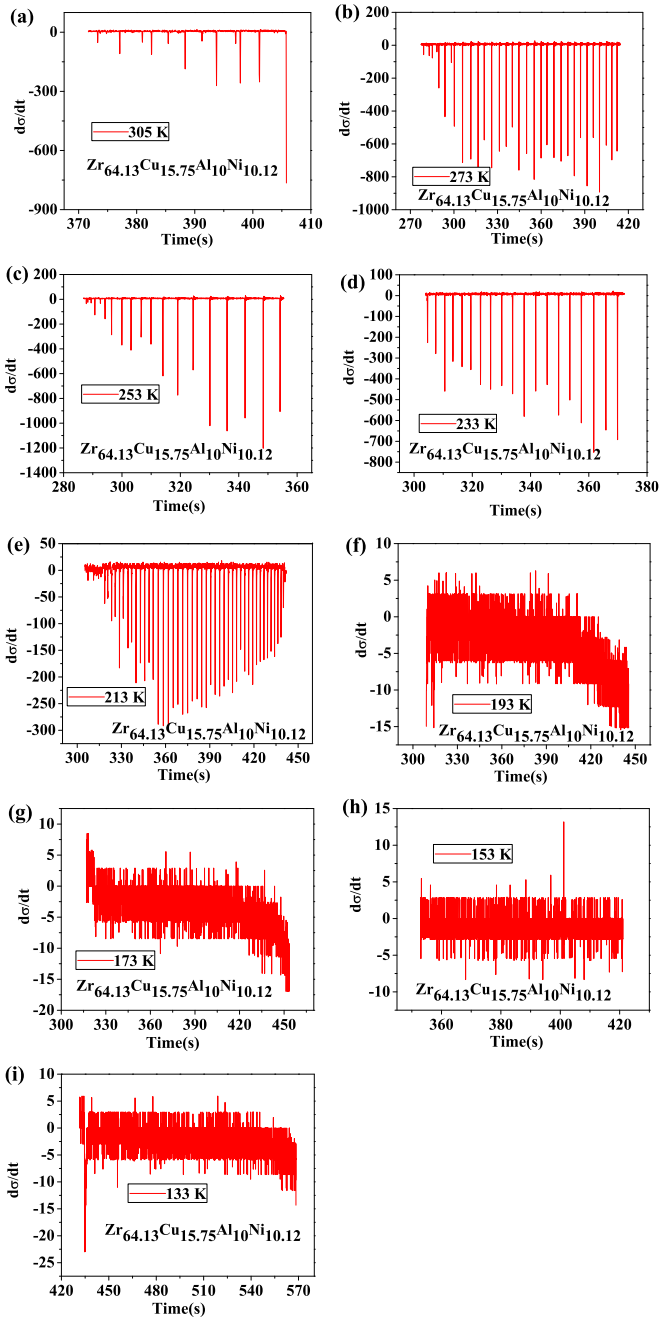

FIG. 2. (Color online) Plot of the stress rate signal $d\sigma/dt$ curves for the $Zr_{64.13}Cu_{15.75}Al_{10}Ni_{10.12}$ glassy metal compressed at a strain rate of $2.5 \times 10^{-4}\ s^{-1}$ at different temperatures, 133, 153, 173, 193, 213, 233, 253, 273, and 305 K. (To clearly show the difference between the results, here we capture part of the overall data.)

where F_q is a power function of the scale q, $F_q \sim q^H$, where H is the Hurst exponent reflecting the long-range memory dependence of the signal.

The Hurst exponent H vs temperature, according to the above detrended fluctuation analysis, is shown in Fig. 3. The Hurst exponent H ranges from 0.11 to 0.48 (see Table I). Here $H \in (0,0.5)$ means a negative correlation and an antipersistent process during the shear-branching process, which implies that the evolution trend of shear branching is opposite to the past

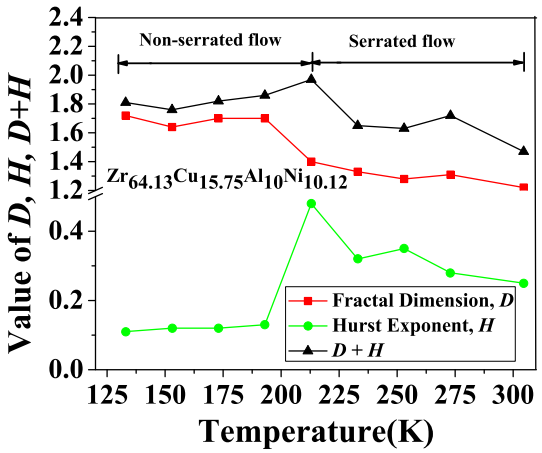

FIG. 3. (Color online) Fractal dimension D [middle (red) line], Hurst exponent H [bottom (green) line], and $D + H$ [top (black) line] of the stress rate signals $d\sigma/dt$ for the $Zr_{64.13}Cu_{15.75}Al_{10}Ni_{10.12}$ glassy metal compressed at a strain rate of $2.5 \times 10^{-4}\,s^{-1}$ and at different temperatures, 133, 153, 173, 193, 213, 233, 253, 273, and 305 K.

progress due to the absence of the long-memory dependence. The stress rate increases persistently over a period of time and then decreases over the next period of time. This trend is consistent with that of the serrated flow, which increases during the elastic energy aggregation and then decreases during the energy release.

As the temperature decreases, the Hurst exponent increases to a maximum value of 0.48 at 213 K and then decreases (see Fig. 3). The maximum Hurst exponent at 213 K reflects that the stress rate signal is a self-similar random process with a weak negative correlation. The shear-branching process behaves like a random walk, which induces homogenization to some degree. On the other hand, a small-H value (such as $H = 0.11$ at 133 K) means a strong negative correlation of the shear-branching process. This strong antipersistent behavior is accompanied by increasing hybridization of shear bands. In this case, the deformation caused by multiple interactions between shear bands is characterized by a low degree of homogenization, i.e., heterogeneity.

An inner correlation between the fractal dimension and Hurst exponent can be described by the modified Cauchy class [28] as a stochastic process. The modified Cauchy class consists of stationary Gaussian random processes $Z(x)$, $x \in R$, which are characterized by their correlation function $c(r) = \langle Z(x), Z(x+r)\rangle$, $x \in R$, and a correlation function satisfying $c(r) = (1 + |r|^{\alpha})^{-(\beta/\alpha)-1}[1 + (1-\beta)|r|^{\alpha}]$, $r \in R$, where $\alpha \in (0,2]$ and $\beta > 1$. The fractal dimension D is given by $D = n + 1 - \alpha/2$ and the Hurst exponent H is given by $H = 1 - \beta/2$. Considering the result that we calculated here, $H \in (0,0.5)$, we give the restriction of $\beta > 1$ in the modified Cauchy class, which can feature the negative correlation of the signal.

TABLE I. Fractal dimension D, Hurst exponent H, values of $D + H$, and E_{approx} of the signal $\{d\sigma(i)/dt,\ i = 1,2,\ldots,N\}$ at different temperatures, 133, 153, 173, 193, 213, 233, 253, 273, and 305 K with a strain rate of $2.5 \times 10^{-4}\,s^{-1}$.

Temperature	133	153	173	193	213	233	253	273	305
D	1.72	1.64	1.7	1.7	1.4	1.33	1.28	1.31	1.22
H	0.11	0.12	0.12	0.13	0.48	0.32	0.35	0.28	0.25
$D + H$	1.83	1.76	1.82	1.83	1.88	1.65	1.63	1.59	1.47
E_{approx}	1.25	1.2	1.3	1.35	0.77	0.21	0.19	0.24	0.48

The stochastic model is suitable for the current situation because not all of the D and H conform to the linear relationship, i.e., $D + H = 2$ (see Fig. 3, the curve of $D + H$ vs temperature). In particular, at a temperature of 213 K, the value of $D + H$ is equal to 1.88 ($\sim$2), which suggests that the signal is close to a self-similar random process. This result is consistent with the above analysis that the Hurst exponent $H = 0.48$ at 213 K, reflecting that the stress rate signal is a self-similar random process with a weak negative correlation. In addition, from Fig. 2, we observe that the signal $\{d\sigma(i)/dt,\ i = 1,2,\ldots,N\}$ is smoothed as the Hurst exponent increases. The tendency here is consistent with the identification of the modified Cauchy class: The closer the Hurst exponent is to 0.5, the smoother the signal curve is [28].

To further characterize the complexity of the system, the concept of entropy is introduced. We can obtain an accurate result about the system by using the approximate entropy (E_{approx}) method [29]. The calculated value of E_{approx} is shown in Table I and E_{approx} as a function of temperature is presented in Fig. 4. A large value of E_{approx} plotted in the low-temperature range suggests that the stress rate signal exhibits a high complexity, which is consistent with the above fractal analysis and the detrended fluctuation analysis. A large fractal dimension at low temperatures reflects the high shear-branching rate with a complex hierarchical structure. A small Hurst exponent (i.e., a strong negative correlation) reflects a low degree of homogenization. The heterogeneity in the stress rate signal induces a disordered and complicated shear-branching process, which can also be observed from the fracture surface.

The activation energy $W = (8/\pi^2)\gamma_c^2 G\Omega$, where G is the shear modulus, Ω is the effective shear transition zone (STZ) volume, and γ_c is a critical shear strain for BMGs ($\gamma_c = 0.036$

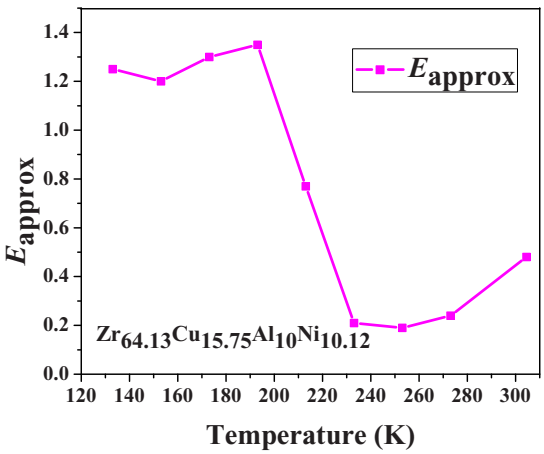

FIG. 4. (Color online) Approximate entropy E_{approx} at different temperatures, 133, 153, 173, 193, 213, 233, 253, 273, and 305 K, with a strain rate of $2.5 \times 10^{-4}\,s^{-1}$.

TABLE II. Mechanical properties of the metallic glass compressed at different temperatures: T is the temperature, G_{0T} is the shear modulus, and τ_{CT} is the critical shear stress.

T (K)	G_{0T} (GPa)	τ_{CT} (MPa)
183	30.2	1087
203	30.0	1080
213	29.9	1076
223	29.8	1073
273	28.9	1040
293	28.5	1026

is found to be a constant for BMGs at room temperature) [30]. The activation volume of the STZ can be calculated by the formula $\Omega = \frac{kT\ln(\omega_0/C\dot{\gamma})}{4RG_{0T}\gamma_{C0}^2\varsigma(1-\tau_{CT}/\tau_{C0})^{3/2}}$ [31], where $\ln(\omega_0/C\dot{\gamma}) \approx 30$, $R \approx 0.25$, $\varsigma \approx 3$; T is the environmental temperature, k is Boltzmann constant (1.381×10^{-23} J/K), τ_{C0} is the yield shear stress at 0 K ($\tau_{C0} = 1124$ MPa), and G_{0T} is the shear modulus at the temperature of T ($G_{0T} = 31.2$ GPa). The critical shear stress τ_{CT} satisfies $\tau_{CT}/G = \gamma_{C0} - \gamma_{C1}(T/T_g)^{2/3}$, where $\gamma_{C0} = 0.036$ and $\gamma_{C1} = 0.016$. The necessary mechanical properties of the $Zr_{64.13}Cu_{15.75}Al_{10}Ni_{10.12}$ BMG compressed at different temperatures are shown in Table II. Based on the above information, the volume and activation energy of the STZ can be calculated (see Fig. 5). The volume of the STZ increases as temperature decreases from 305 to 133 K; the activation energy of the STZ increases correspondingly. This result is consistent with the calculation results of the E_{approx} value, i.e., the increased complexity of the shear-branching process appearing at low temperature. The larger fractal dimension reflects the more complex hierarchical structure of the shear-branching process at lower temperatures. The high complexity of the shear-branching process at low temperature confirms theoretically that there is a large activation energy used for activating the STZ, which facilitates the plastic flow of BMGs.

In summary, the self-similar behavior and complexity in the temporal scale of the stress rate signal have been investigated at temperatures well below the glass-transition temperature. The obvious fractal behavior suggests that the shear-banding process is accompanied by larger branching rates from a primary shear band to a secondary shear band. In fact, at a temperature of 133 K, many shear bands interact with each other and the sample contains more elastic energy, which is facilitated to produce the good plasticity of metallic glasses. A Cauchy class model was introduced for the stochastic shear-branching process, which connects the fractal dimension and Hurst exponent and features the negative correlation process. In addition, the Hurst exponent reaches a maximum value of 0.48 at a temperature of 213 K; in particular, at a temperature of 213 K, the value of $D + H$ approaches 2, suggesting that

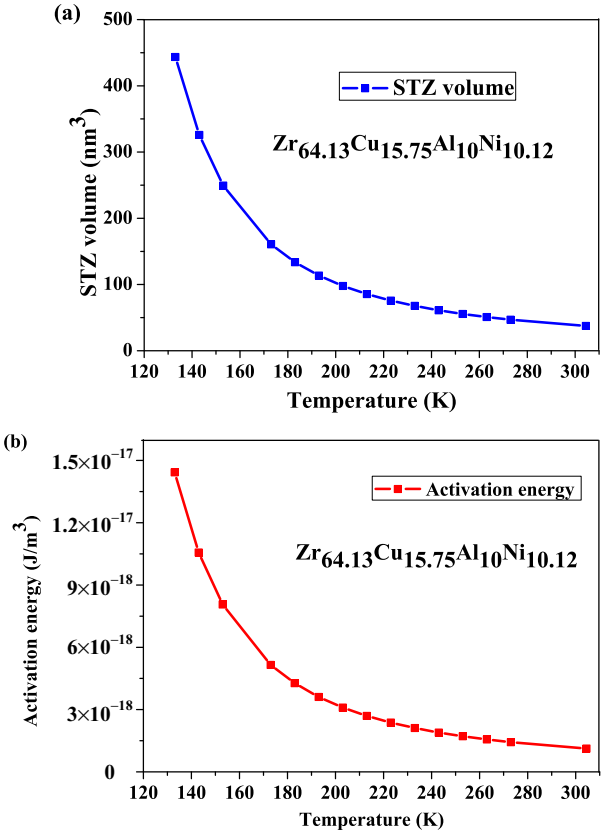

FIG. 5. (Color online) (a) Volume of STZ at different temperatures and (b) activation energies at different temperatures, 133, 153, 173, 193, 213, 233, 253, 273, and 305 K.

the shear-branching process evolves as a self-similar random process, which induces a degree of homogenization in shear bands. Furthermore, the analysis of approximate entropy suggests that there is a complicated hierarchy structure at low temperatures, which can be interpreted as there being many shear bands interacting at lower temperatures, which induces a SOC state. We have given an explanation of the superplasticity of the BMGs from the perspective of the temporal scaling behavior and the complexity at low temperature.

This work was supported by the NSFC (Grants No. 11271339, No. 51171098, and No. 51222102) and the ZDGD13001 program. P.K.L. very much appreciates financial support from the U.S. National Science Foundation (Grant No. CMMI-1100080). K.A.D. and P.K.L. are very grateful for the support from the US Department of Energy, Office of Fossil Energy, National Energy Technology Laboratory (Grants No. DE-FE-0008855, No. DE-FE-0011194, and No. DE-FE-0024054), and the U.S. Army Research Office (Grant No. W911NF-13-1-0438).

[1] R. Sarmah, G. Ananthakrishna, B. A. Sun, and W. H. Wang, Hidden order in serrated flow of metallic glasses, Acta Mater. **59**, 4482 (2011).

[2] G. Wang, K. C. Chan, L. Xia, P. Yu, J. Shen, and W. H. Wang, Self-organized intermittent plastic flow in bulk metallic glasses, Acta Mater. **57**, 6146 (2009).

[3] J. L. Ren, C. Chen, G. Wang, N. Mattern, and J. Eckert, Dynamics of serrated flow in a bulk metallic glass, AIP Adv. **1**, 032158 (2011).

[4] J. L. Ren, C. Chen, Z. Y. Liu, R. Li, and G. Wang, Plastic dynamics transition between chaotic and self-organized critical states in a glassy metal via a multifractal intermediate, Phys. Rev. B **86**, 134303 (2012).

[5] Y. Q. Cheng, Z. Han, Y. Li, and E. Ma, Cold versus hot shear banding in bulk metallic glass, Phys. Rev. B **80**, 134115 (2009).

[6] B. A. Sun, H. B. Yu, W. Jiao, H. Y. Bai, D. Q. Zhao, and W. H. Wang, Plasticity of ductile metallic glasses: A self-organized critical state, Phys. Rev. Lett. **105**, 035501 (2010).

[7] B. A. Sun, S. Pauly, J. Tan, M. Stoica, W. H. Wang, U. Kühn, and J. Eckert, Serrated flow and stick–slip deformation dynamics in the presence of shear-band interactions for a Zr-based metallic glass, Acta Mater. **60**, 4160 (2012).

[8] J. L. Ren, C. Chen, G. Wang, W. S. Cheung, B. A. Sun, N. Mattern, S. Siegmund, and J. Eckert, Various sizes of sliding event bursts in the plastic flow of metallic glasses based on a spatiotemporal dynamic model, J. Appl. Phys. **116**, 033520 (2014).

[9] J. Antonaglia, W. J. Wright, X. J. Gu, R. R. Byer, T. C. Hufnagel, M. LeBlanc, J. T. Uhl, and K. A. Dahmen, Bulk metallic glasses deform via slip avalanches, Phys. Rev. Lett. **112**, 155501 (2014).

[10] J. Antonaglia, X. Xie, G. Schwarz, M. Wraith, J. W. Qiao, Y. Zhang, P. K. Liaw, J. T. Uhl, and K. A. Dahmen, Tuned critical avalanche scaling in bulk metallic glasses, Sci. Rep. **4**, 4382 (2014).

[11] B. A. Sun and W. H. Wang, Fractal nature of multiple shear bands in severely deformed metallic glass, Appl. Phys. Lett. **98**, 201902 (2011).

[12] Z. Y. Liu, G. Wang, K. C. Chan, J. L. Ren, Y. L. Huang, X. L. Bian, X. H. Xu, D. S. Zhang, Y. L. Gao, and Q. J. Zhai, Temperature dependent dynamics transition of intermittent plastic flow in a metallic glass. I. Experimental investigations, J. Appl. Phys. **114**, 033520 (2013).

[13] Z. Wang, B. A. Sun, H. Y. Bai, and W. H. Wang, Evolution of hidden localized flow during glass-to-liquid transition in metallic glass, Nat. Commun. **5**, 5823 (2014).

[14] W. H. Jiang, F. X. Liu, D. C. Qiao, H. Choo, and P. K. Liaw, Plastic flow in dynamic compression of a Zr-based bulk metallic glass, J. Mater. Res. **21**, 1570 (2006).

[15] D. Klaumünzer, R. Maaß, F. H. Dalla Torre, and J. F. Löffler, Temperature-dependent shear band dynamics in a Zr-based bulk metallic glass, Appl. Phys. Lett. **96**, 061901 (2010).

[16] W. H. Jiang, G. J. Fan, F. X. Liu, G. Y. Wang, H. Choo, and P. K. Liaw, Spatiotemporally inhomogeneous plastic flow of a bulk-metallic glass, Int. J. Plasticity **24**, 1 (2008).

[17] J. Tan, G. Wang, Z. Y. Liu, J. Bednarčík, Y. L. Gao, Q. J. Zhai, N. Mattern, and J. Eckert, Correlation between atomic structure evolution and strength in a bulk metallic glass at cryogenic temperature, Sci. Rep. **4**, 3897 (2014).

[18] D. B. Miracle, A structural model for metallic glasses, Nat. Mater. **3**, 697 (2004).

[19] D. B. Miracle, The efficient cluster packing model - An atomic structural model for metallic glasses, Acta Mater. **54**, 4317 (2006).

[20] H. W. Sheng, W. K. Luo, F. M. Alamgir, J. M. Bai, and E. Ma, Atomic packing and short-to-medium-range order in metallic glasses, Nature (London) **439**, 419 (2006).

[21] D. Ma, A. D. Stoica, and X. L.Wang, Power-law scaling and fractal nature of medium-range order in metallic glasses, Nat. Mater. **8**, 30 (2009).

[22] X. K. Xi, D. Q. Zhao, M. X. Pan, W. H. Wang, Y. Wu, and J. J. Lewandowski, Fracture of brittle metallic glasses: Brittleness or plasticity, Phys. Rev. Lett. **94**, 125510 (2005).

[23] T. Vicsek, *Fractal Growth Phenomena* (World Scientific, Singapore, 1992).

[24] C. K. Peng, J. Mietus, J. M. Hausdorff, S. Havlin, H. E. Stanley, and A. L. Goldberger, Long-range anti-correlations and non-Gaussian behavior of the heartbeat, Phys. Rev. Lett. **70**, 1343 (1993).

[25] C. K. Peng, S. V. Buldyrev, S. Havlin, M. Simons, H. E. Stanley, and A. L. Goldberger, Mosaic organization of DNA nucleotides, Phys. Rev. E **49**, 1685 (1994).

[26] K. Hu, P. Ch. Ivanov, Z. Chen, P. Carpena, and H. E. Stanley, Effect of trends on detrended fluctuation analysis, Phys. Rev. E **64**, 011114 (2001).

[27] Z. Chen, P. Ch. Ivanov, K. Hu, and H. E. Stanley, Effect of nonstationarities on detrended fluctuation analysis, Phys. Rev. E **65**, 041107 (2002).

[28] T. Gneiting and M. Schlather, Stochastic models that separate fractal dimension and the Hurst effect, SIAM Rev. **46**, 269 (2004).

[29] S. M. Pincus, Approximate entropy as a measure of system complexity, Proc. Natl. Acad. Sci. USA **88**, 2297 (1991).

[30] M. D. Demetriou, J. S. Harmon, M. Tao, G. Duan, K. Samwer, and W. L. Johnson, Cooperative shear model for the rheology of glass-forming metallic liquids, Phys. Rev. Lett. **97**, 065502 (2006).

[31] W. L. Johnson and K. Samwer, A universal criterion for plastic yielding of metallic glasses with a $(T/T_g)^{2/3}$ temperature dependenc, Phys. Rev. Lett. **95**, 195501 (2005).